

# Optical, structural and electrical investigations on $\text{PbTe}_{1-x}\text{S}_x$ alloys

Sushil Kumar · M. A. Majeed Khan ·  
M. Zulfequar · M. Husain

Received: 28 September 2004 / Accepted: 13 July 2005 / Published online: 29 November 2006  
© Springer Science+Business Media, LLC 2006

**Abstract** The fabrication of devices with lead salts and their alloys with detecting and lasing capabilities has been an important technological development. The high quality polycrystalline thin films of  $\text{PbTe}_{1-x}\text{S}_x$  with variable composition ( $0 \leq x \leq 1$ ) have been deposited onto ultra clean glass substrates by vacuum evaporation technique. Optical, structural and electrical properties of  $\text{PbTe}_{1-x}\text{S}_x$  thin films have been examined. Absorption coefficient and band gap of the films were determined by absorbance measurements in wavelength range 2,500–5,000 nm using FTIR spectrophotometer. Sample nature, crystal structure and lattice parameter of the films were determined from X-ray diffraction patterns. DC conductivity and activation energy of the films were measured in temperature range 300–380 K through I–V measurements.

## Introduction

IV–VI compounds [1, 2] have been the subject of considerable attention, owing to their technological importance in the IR field. The fabrication of devices with alloys of these compounds with photodetection and injection laser capabilities has been an important technological development [3, 4]. They have been

applied in long wavelength imaging [5], diode lasers [6], and in thermophotovoltaic energy converters [7]. Of great interest is their application in the fields of gas spectroscopy and pollution control [8], remote sensing, thermography, chemical sensing [9] etc.

The development of laser technology has opened up new applications for IV–VI compounds. The laser diodes based on lead chalcogenides and their alloys are important sources for the tunable radiations in the mid infrared wavelength region. They are considered to be mainly utilized to an advanced measurement system for detecting hydrocarbon pollutants in atmosphere, high-resolution spectroscopy, trace gas analysis and also to a new optical fibre communication system over super long distances [10, 11]. The narrow gap IV–VI semiconductors have been the subject of extensive research [12] as they are suited for the fabrication of photovoltaic infrared sensors. Photovoltaic IV–VI infrared sensors ( $\text{Pb}_{1-x}\text{Sn}_x\text{Te}$ ,  $\text{Pb}_{1-x}\text{Sn}_x\text{Se}$ ,  $\text{PbS}_{1-x}\text{Se}_x$ ,  $\text{PbTe}$  etc.) offer similar sensitivities as  $\text{Hg}_{1-x}\text{Cd}_x\text{Te}$ , and are much easier to fabricate especially as their layers on Si substrates. However, the technology of photovoltaic lead salts arrays is behind that of  $\text{Hg}_{1-x}\text{Cd}_x\text{Te}$  [13–18].

Thin film polycrystalline semiconductors has attracted much interest in an expanding variety of applications in various electronic and optoelectronic devices. The technological interest in polycrystalline based devices is mainly caused by their very low production costs. Many of the significant advances taken place in recent years have been mainly due to the ability to prepare not only structurally and chemically pure crystals but also crystals with a controlled impurity. The role that thin films have played in some of these advances is well established [19–22].

S. Kumar · M. A. Majeed Khan · M. Zulfequar ·  
M. Husain (✉)  
Department of Physics, Jamia Millia Islamia, New Delhi  
110025, India  
e-mail: Mush\_phys@rediffmail.com

## Experimental

In the present research work, quenching method has been adopted to prepare the polycrystalline  $\text{PbTe}_{1-x}\text{S}_x$  alloys. Highly pure materials 99.999% having desired compositional ratio of elements were sealed in quartz ampoules (length ~12 cm, internal diameter ~0.8 cm) in a vacuum of about  $10^{-6}$  torr. The sealed ampoules were kept inside a programmable furnace where the temperature was raised upto 800 °C at a rate of 4 °C per min. and then maintained it for 10 h. The ampoules were rocked frequently to ensure the homogenization of the melt. The ampoules having the material in molten state (stoichiometric melt) were allowed to cool down to room temperature in the furnace by switching off the furnace. The ingots of the sample were taken out and grinded into fine powder. The polycrystalline nature of the samples was confirmed by X-ray diffraction (Fig. 1).

The good quality polycrystalline thin films of thickness 500 nm were deposited on ultra clean glass substrates by vacuum evaporation technique keeping the substrates at room temperature in a vacuum of  $10^{-5}$  torr. The deposited films were annealed in the same vacuum chamber at about 80 °C for 2 h. The films were kept inside the vacuum chamber for 24 h to attain metastable equilibrium as suggested by Abkowitz [23]. Thickness of the films has been measured using quartz crystal thickness monitor. Deposition parameters were kept same for all the films.

The absorbance spectra of the thin films of  $\text{PbTe}_{1-x}\text{S}_x$  system were measured in wavelength range 2,500–5,000 nm using Fourier transform infrared spectrophotometer (Nicolet, Impact, model 410). A Philips PW 1140/09 X-ray diffractometer was employed for studying the structure of thin films. The copper target was used as a source of X-rays with  $\lambda = 1.5405 \text{ \AA}$  ( $\text{Cu K}\alpha_1$ ). The scanning angle was in the range of  $10^\circ$ – $90^\circ$ . A scan speed of  $2^\circ/\text{min}$  and a chart speed of  $1 \text{ cm}/\text{min}$ . were maintained. For electrical conductivity, the narrow films were deposited on glass substrates on which indium electrodes with gap were pre-deposited. The dc conductivity of the films was measured in temperature range 300–380 K.

The electrical measurements have been carried out in a vacuum of  $10^{-3}$  torr in a specially designed sample holder. For low field measurements, a dc voltage source in the form of a dry cell of 1.5 V has been used. The temperature of the film is measured by a copper-constantan thermocouple and was increased by a step value of 2.5 °C and correspondingly the current was measured by an electrometer (Keithley, model 617).

## Results and discussion

### Optical characterization

The absorbance spectra of the thin films of  $\text{PbTe}_{1-x}\text{S}_x$  alloys were studied to evaluate the absorption coefficient ( $\alpha$ ) and bandgap ( $E_g$ ). The absorption coefficient can be derived from the absorbance  $A$ , which is the ratio  $I_0/I_t$ , where  $I_0$  is the incident intensity and  $I_t$  is the intensity after traversing a thickness  $t$  in the sample [24–29]

absorption coefficient = optical density/thickness

$$\alpha = (1/t) \log(I_0/I_t). \quad (1)$$

The various types of transitions give rise to different frequency dependencies of the absorption coefficient near the fundamental absorption edge. The absorption coefficient can also be given by [1, 30]

$$\alpha(h\nu) = A^*(h\nu - E_g)^m \text{ cm}^{-1}. \quad (2)$$

For allowed direct transitions  $m = 1/2$  and  $A^*$  is constant.  $h\nu$  and  $E_g$  being expressed in eV. Plotting  $(\alpha h\nu)^2$  along ordinate axis and  $h\nu$  along abscissa, we obtained straight line whose intercept on abscissa is equal to the forbidden bandwidth of the sample. In case of lead salts the maxima of valence band and the minima of conduction band lie at the same  $k$  value of  $E$ – $k$  band diagram and hence the transitions are direct type.

From the variation of the absorption coefficient as a function of wavelength for  $\text{PbTe}_{1-x}\text{S}_x$  alloys (Figure not shown here), it is observed that the absorption coefficient is high ( $\approx 10^4 \text{ cm}^{-1}$ ) and increases sharply below a certain wavelength, for all the compositions of the system. Near the fundamental absorption edge, the absorption coefficient varies rapidly with wavelength (frequency). The absorption edge shifts towards the shorter wavelength as  $x$  increases from 0 to 1.

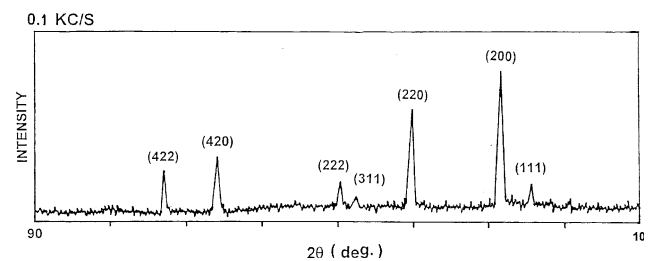


**Fig. 1** X-ray diffraction pattern of  $\text{PbTe}_{0.8}\text{S}_{0.2}$  film

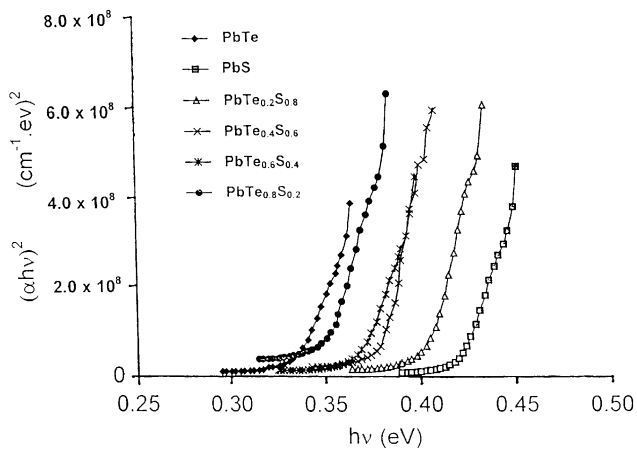


**Fig. 2**  $(\alpha hv)^2$  vs.  $h\nu$  graph for PbTe<sub>1-x</sub>S<sub>x</sub> films

The variation of  $(\alpha hv)^2$  with  $h\nu$  for PbTe<sub>1-x</sub>S<sub>x</sub> films is shown in Fig. 2. It has been observed that the plots of  $(\alpha hv)^2$  versus  $h\nu$  are linear over a wide range of photon energies indicating the direct type of transitions. The intercepts (extrapolations) of these plots (straight lines) on the energy axis give the energy band gaps. The band gaps for all the compositions were determined. The band gap changes from 0.33 to 0.42 eV as  $x$  changes from 0 to 1. The compositional dependence of the band gap is given in Table 1. The variation of  $E_g$  with  $x$  is almost linear for this system. It was established experimentally that the dependence of the bandgap on the composition  $E_g(x)$  for the majority of the investigated and widely used solid solutions based on IV–VI compounds is quite accurately linear [31].

**Structural characterization**

The X-ray diffraction patterns give valuable information about the nature and structure of the samples. The X-ray diffraction traces of all samples were taken at room temperature and found to show almost similar trends and hence only one of them (for PbTe<sub>0.8</sub>S<sub>0.2</sub>) is shown in Fig. 1. The presence of sharp structural peaks in these XRD traces confirmed the polycrystalline nature of the samples. The  $d$ -values are experimentally

determined from the Bragg’s relation  $2d_{hkl} \sin\theta = n\lambda$  (in our case  $n = 1$ ,  $\lambda = 1.5405 \text{ \AA}$ ) by taking  $\theta$ -values from the peaks of XRD pattern.

Vegard’s law states that the value of the lattice parameters of an alloy as obtained by X-ray data, are the linear function of concentrations of the constituent crystals and are expressed as [32]

$$r = \lambda_1 r_1 + \lambda_2 r_2 \tag{3}$$

where  $r_1$  and  $r_2$  are the lattice parameters of the constituent crystals and  $r$  that of the alloy.  $\lambda_1$  and  $\lambda_2$  are the mole fractions of the constituent crystals.

The  $d$ -values are in good agreement with the ASTM data or data obtained from Vegard’s law for the PbTe<sub>1-x</sub>S<sub>x</sub> system confirming the rock salt (NaCl) structure of these alloys of lead chalcogenides.

The lattice constants can be determined by combining the Bragg’s law and the plane-spacing equation for cubic crystal [33]

$$\sin^2 \theta_{hkl} = (\lambda^2/4a^2) (h^2 + k^2 + l^2). \tag{4}$$

This equation predicts, for a particular incident wavelength  $\lambda$  and a particular cubic crystal of unit cell size  $a$ , all the possible Bragg angles at which diffraction can occur from the planes ( $hkl$ ).

For each composition of these alloys of lead chalcogenides, the peak intensity of X-ray diffracted beam is obtained for (200) plane. The lattice constant ( $a$ ) and plane spacing ( $d$ ) calculated for each of these different compositions is shown in Table 1. The lattice parameters of each composition of ternary alloys of PbTe<sub>1-x</sub>S<sub>x</sub> follow the Vegard’s law meaning that within the experimental errors, the lattice parameter of these ternary alloys of concentration  $x$  can be linearly interpolated from the lattice constants of the corresponding lead salts.

**Electrical characterization**

Conductivity is an important factor which reveals the important and reliable information about the transport

**Table 1** Optical, structural and electrical parameters of PbTe<sub>1-x</sub>S<sub>x</sub> alloys

S. No.	Compound/alloy	Composition	$E_g$ (eV)	$a$ (Å)	$d$ (Å)	$\sigma_{dc}$ ( $T = 350 \text{ K}$ ) ( $\Omega^{-1}\text{cm}^{-1}$ )	$\Delta E$ (eV)
1.	PbTe	0	0.33	6.470	3.235	$2.37 \times 10^{-5}$	0.11
2.	PbTe <sub>0.8</sub> S <sub>0.2</sub>	0.2	0.35	6.334	3.167	$1.78 \times 10^{-5}$	0.08
3.	PbTe <sub>0.6</sub> S <sub>0.4</sub>	0.4	0.37	6.237	3.118	$1.29 \times 10^{-5}$	0.19
4.	PbTe <sub>0.4</sub> S <sub>0.6</sub>	0.6	0.38	6.133	3.066	$0.78 \times 10^{-5}$	0.23
5.	PbTe <sub>0.2</sub> S <sub>0.8</sub>	0.8	0.40	6.041	3.021	$0.40 \times 10^{-5}$	0.13
6.	PbS	1	0.42	5.952	2.976	$0.01 \times 10^{-5}$	0.20

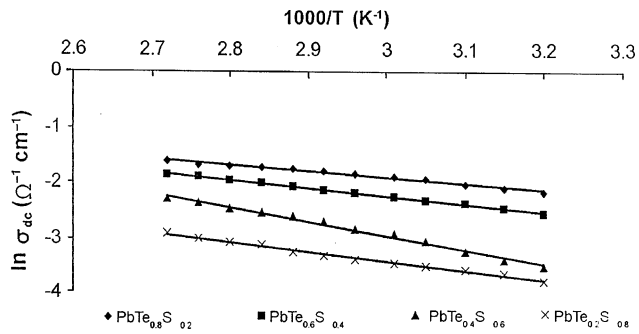


**Fig. 3** Plot of  $\ln \sigma_{dc}$  vs.  $1,000/T$  for  $\text{PbTe}_{1-x}\text{S}_x$  films

phenomenon of the materials. The dc electrical conductivity of a semiconductor at temperature  $T$  is given by

$$\sigma_{dc} = \sigma_0 \exp(-\Delta E/kT) \quad (5)$$

where  $\Delta E$  is the activation energy for the generation process and  $k$  is the Boltzmann constant. We may write

$$\ln \sigma_{dc} = -(\Delta E/1,000k) \cdot (1,000/T) + \ln \sigma_0. \quad (6)$$

When we plot a graph between  $\ln \sigma_{dc}$  and  $1,000/T$ , a straight line is obtained having slope  $(\Delta E/1,000k)$  and intercept  $\ln \sigma_0$ .

The thin films of the present system of  $\text{PbTe}_{1-x}\text{S}_x$  alloys are studied for their dc conductivity ( $\sigma_{dc}$ ) and activation energy ( $\Delta E$ ) in the temperature range 300–380 K. Figure 3 shows the temperature dependence of dark conductivity for  $\text{PbTe}_{1-x}\text{S}_x$  alloys. The conductivity of all these samples increases with increase in temperature showing the semiconducting behaviour of these alloys. The plots of  $\ln \sigma_{dc}$  against  $1,000/T$  are straight lines for all the samples indicating that conduction in these samples is through thermally activated process. The results of other workers [34, 35] on the polycrystalline films of lead chalcogenides support the thermally activated conduction. The activation energy for these alloys have been calculated by using the slope of the curve plotted between  $\ln \sigma_{dc}$  and  $1,000/T$ . The variation of dc conductivity and activation energy with composition ( $x$ ) are given in Table 1. It has been observed that dc conductivity decreases as  $x$  increases from 0 to 1 for  $\text{PbTe}_{1-x}\text{S}_x$  alloys. The activation energy of different compositions of this system is of the order of  $10^{-1}$  eV.

## Conclusion

In view of the fact that pseudo-binaries of lead chalcogenides form well miscible solid solutions over

a wide composition range, the recent trend in this field has been the preparation and characterization of polycrystalline ternary composition like lead telluride sulphide for device fabrication. Tailoring of band gap through variation of composition has enabled the fabrication of detectors and tunable emitters of coherent radiations. All the films were found to be polycrystalline in nature as confirmed by XRD patterns and have a predominantly rock salt (NaCl) structure. The electrical conduction process in the films is through thermally activated process.

**Acknowledgement** The financial support from the Council of Scientific and Industrial Research, New Delhi (India) is gratefully acknowledged.

## References

1. Ravich Yu I, Effimova BA, Smirnov IA (1970) Semiconducting lead chalcogenides. Plenum Press, New York
2. Zemel JN (1969) Solid State Surf Sci 1:291
3. Proc. IEEE 63 (1) (1975)
4. Hesse J, Prier H (1975) Festkörperprobleme 15:229
5. Zogg H, Fach A, John J, Masek J, Muller P, Paglino C, Buttler W (1994) Opt Eng 33:1440
6. Preier H (1979) Appl Phys 20:189
7. Chaudhuri TK (1992) Int J Engg Res 16:481
8. Abbe S, Furukawa Y, Mochizuki K, Masumato K (1994) J Jpn Inst Metals 58:346
9. Zemel JN (1975) In: Scott CG, Reed CE (eds) Surface physics of phosphors and semiconductors. Academic Press, London, pp 523–562
10. Lambrecht A, Kurbel R, Agne M (1993) Mater Sci Eng 21:217
11. Agne M, Lambrecht A, Schiessl U, Tacke M (1994) Infrared Phys Technol 35:47
12. Carter DL, Bates RT (eds) (1971) The physics of semimetals and narrow gap semiconductors. Pergamon, New York
13. Fach A, John J, Muller P, Paglino C, Zogg H (1997) J Electron Mater 26:873
14. John J, Zogg H (1999) J Appl Phys 85:1
15. Paglino C, Fach A, John J, Muller P, Zogg H (1996) J Appl Phys 80:7138
16. Rogalski A (1995) Infrared photon detectors. SPIE Optical Engineering Press, Bellingham, WA
17. Holloway H (1980) Physics of thin films, vol 11. Academic Press, pp 105–203
18. Adamiec K, Rogalski A, Rutkowski J (1997) J Tech Phys 38:431
19. Maissel LI, Glang R (eds) (1970) Handbook of thin film technology. McGraw Hill, New York
20. Mathews JW (ed) (1975) Epitaxial growth. Academic Press, New York
21. Anderson JC (ed) (1966) The use of thin films in physical investigations. Academic Press, New York
22. Chopra KL (1969) Thin film phenomena. McGraw Hill, New York
23. Abkowitz M (1984) Polym Engg Sci 24:1149
24. Rubin KA, Chen M (1989) Thin Solid Films 181:129
25. Maeda Y, Andoh H, Ikuta I, Minemura H (1988) Appl Opt 64:1715

26. Gosain DP, Shimizu I, Ohmura M, Suzuki M, Bando T, Okano S (1991) *J Mater Sci* 26:3271
27. Gravesteiju DJ (1988) *Appl Opt* 27:736
28. Shokr EK, Wakkad MM (1992) *J Mater Sci* 27:1197
29. Oe K, Toyoshima Y, Nagai H (1976) *J Non-crystalline Solids* 20:405
30. Pankove JI (1971) *Optical processes in semiconductors*. Prentice-Hall Inc, New Jersey
31. Harman TC, Melngailis I (1974) *Appl Solid State Sci* 4:1
32. Bis RF, Dixon JR (1969) *J Appl Phys* 40:1918
33. Cullity BD (1959) *Elements of X-ray diffraction*. Addison-Wesley Publishing Co. Inc, Massachusetts/London
34. Espevick S, Wu Chen-ho, Bube RH (1971) *J Appl Phys* 42:3513
35. Briones F, Galmayo D, Ortiz C (1981) *Thin Solid Films* 78:385